

# Acoustic surface plasmons in the noble metals Cu, Ag, and Au

V. M. Silkin,<sup>1</sup> J. M. Pitarke,<sup>1,2</sup> E. V. Chulkov,<sup>1,3</sup> and P. M. Echenique<sup>1,3</sup>

<sup>1</sup>*Donostia International Physics Center (DIPC),*

*Manuel de Lardizabal Pasealekua, E-20018 Donostia, Basque Country, Spain*

<sup>2</sup>*Materia Kondentsatuaren Fisika Saila, Zientzi Fakultatea, Euskal Herriko Unibertsitatea, 644 Posta kutxatila, E-48080 Bilbo, Basque Country, Spain*

<sup>3</sup>*Materialen Fisika Saila, Kimika Fakultatea, Euskal Herriko Unibertsitatea and Centro Mixto CSIC-UPV/EHU 1072 Posta kutxatila, E-20080 Donostia, Basque Country, Spain*

(Dated: June 26, 2021)

We have performed self-consistent calculations of the dynamical response of the (111) surface of the noble metals Cu, Ag, and Au. Our results indicate that the partially occupied surface-state band in these materials yields the existence of acoustic surface plasmons with linear dispersion at small wave vectors. Here we demonstrate that the sound velocity of these low-energy collective excitations, which had already been predicted to exist in the case of Be(0001), is dictated not only by the Fermi velocity of the two-dimensional surface-state band but also by the nature of the decay and penetration of the surface-state orbitals into the solid. Our linewidth calculations indicate that acoustic surface plasmons should be well defined in the energy range from zero to  $\sim 400$  meV.

PACS numbers: 71.45.Gm, 73.20.At

## I. INTRODUCTION

During the last decades a variety of metal surfaces, such as Be(0001) and the (111) surfaces of the noble metals Cu, Ag, and Au, have become a testing ground for many experimental and theoretical investigations.<sup>1,2,3,4</sup> These surfaces are known to support a partially occupied band of Shockley surface states with energies near the Fermi level. Since these states are strongly localized near the surface and disperse with momentum parallel to the surface, they can be considered to form a quasi two-dimensional (2D) surface-state band with a 2D Fermi energy  $\varepsilon_F^{2D}$  equal to the surface-state binding energy at the  $\Gamma$  point.

In the absence of the three-dimensional (3D) substrate, partially occupied Shockley surface states would support a 2D collective oscillation, the energy of this plasmon being given by (unless stated otherwise, atomic units are used, i.e.,  $e^2 = \hbar = m_e = 1$ )<sup>5,6</sup>

$$\omega_{2D} = \sqrt{2\pi n_{2D}q/m_{2D}}, \quad (1)$$

where  $n_{2D}$  represents the density of occupied surface states:  $n_{2D} = \varepsilon_F^{2D}/\pi$ ,  $q$  represents the magnitude of a 2D wave vector, and  $m_{2D}$  is a 2D effective mass. Eq. (1) shows that at very long wavelengths plasmons in a 2D electron gas have low energies; however, they do not affect electron-hole (e-h) and phonon dynamics near the Fermi level, due to their square-root dependence on the wave vector. Much more effective than ordinary 2D plasmons in mediating, e.g., superconductivity would be the so-called acoustic plasmons with sound-like long-wavelength dispersion.<sup>7</sup>

Recently, it has been demonstrated that in the presence of the 3D substrate the dynamical screening at the surface provides a mechanism for the existence of a *new* acoustic collective mode, whose energy exhibits a linear dependence on the 2D wave vector.<sup>8,9</sup> We refer to this

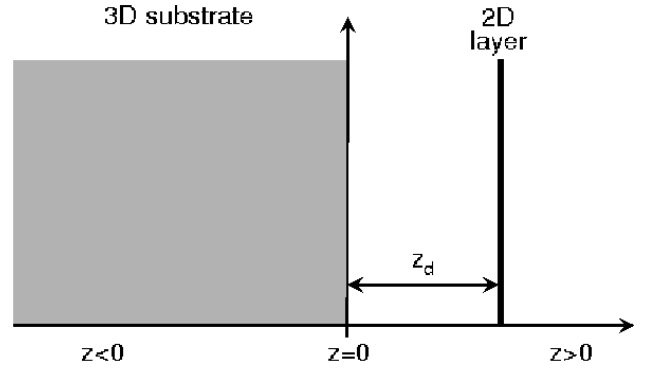


FIG. 1: Simplified model in which surface-state electrons comprise a 2D sheet of interacting free electrons at  $z = z_d$ . All other states of the semi-infinite metal are assumed to comprise a plane-bounded 3D electron gas at  $z \leq 0$ . The metal surface is located at  $z = 0$ .

mode as *acoustic surface plasmon* (ASP), to distinguish it from the conventional surface plasmon predicted by Ritchie.<sup>10</sup> The energy of this latter plasmon is known to be  $\omega_s = \omega_p/\sqrt{2}$ , where  $\omega_p$  is the plasmon energy of a homogeneous electron gas of density  $n_0$ :  $\omega_p = (4\pi n_0)^{1/2}$ .

In a simplified model in which surface-state electrons comprise a 2D electron gas at  $z = z_d$  (see Fig. 1), while all other states of the semi-infinite metal comprise a 3D substrate at  $z \leq 0$ , one finds that both e-h and collective excitations occurring within the 2D gas can be described with the use of an effective 2D dielectric function, which in the random-phase approximation (RPA) takes the form<sup>9</sup>

$$\epsilon_{eff}(q, \omega) = 1 - W(z_d, z_d; q, \omega) \chi_{2D}^0(q, \omega), \quad (2)$$

$W(z, z'; q, \omega)$  being the 2D Fourier transform of the so-called screened interaction in the presence of the 3D substrate alone,<sup>11</sup> and  $\chi_{2D}^0(q, \omega)$  being the noninteracting density-response function of a 2D electron gas.<sup>5</sup>

In the absence of the 3D substrate,  $W(z, z'; q, \omega)$  yields the 2D Fourier transform of the bare Coulomb interaction and  $\epsilon_{eff}(q, \omega)$  coincides, therefore, with the RPA dielectric function of a 2D electron gas, which in the long-wavelength ( $q \rightarrow 0$ ) limit has one single zero corresponding to collective oscillations at  $\omega = \omega_{2D}$ .

In the presence of a 3D substrate, the long-wavelength limit of  $\epsilon_{eff}(q, \omega)$  has two zeros.<sup>12</sup> One zero corresponds to a high-frequency oscillation of energy  $\omega^2 = \omega_s^2 + \omega_{2D}^2$  in which 2D and 3D electrons oscillate in phase with one another. The other zero corresponds to a low-frequency *acoustic* oscillation in which 2D and 3D electrons oscillate out of phase. The energy of this low-frequency mode is found to be of the form<sup>9</sup>

$$\omega = \alpha v_F^{2D} q, \quad (3)$$

where  $v_F^{2D}$  represents the 2D Fermi velocity

$$v_F^{2D} = \sqrt{2\varepsilon_F^{2D}/m_{2D}}, \quad (4)$$

and

$$\alpha = \sqrt{1 + \frac{[I(z_d)]^2}{\pi[\pi + 2I(z_d)]}}, \quad (5)$$

with

$$I(z_d) = \lim_{q \rightarrow 0} W(z_d, z_d; q, \alpha v_F^{2D} q). \quad (6)$$

The coefficient  $\alpha$  (whose value depends on the electron density of the 3D substrate and increases with  $z_d$ ) ranges from a constant value (on the order of 1.3–1.6 for metallic densities) for a 2D sheet far inside the 3D substrate to the asymptotic value  $\sqrt{2z_d}$  (see Ref. 13) for a 2D sheet far outside the metal surface.

In this paper, we extend the self-consistent calculations of the dynamical response of Be(001) reported in Ref. 8 to the case of the (111) surface of the noble metals Cu, Ag, and Au. Our results indicate that the partially occupied surface-state band in these materials yields the existence of acoustic surface plasmons whose energy is of the form of Eq. (3), but with an  $\alpha$  coefficient that is much closer to unity than expected from the simplified model described above. Furthermore, we demonstrate that the sound velocity ( $v_s = \alpha v_F^{2D}$ ) of this low-energy collective excitation is dictated not only by the Fermi velocity of the 2D surface-state band but also by the nature of the decay and penetration of the surface-state orbitals into the solid. We also investigate the width of the corresponding plasmon peak, which dictates the lifetime of this collective excitation.

## II. THEORY

In order to achieve a full description of the dynamical response of real metal surfaces, we first consider the

one-dimensional potential of Ref. 14. This allows us to assume translational invariance in the plane of the surface, which yields, within linear-response theory, the following expression for the electron density induced by an external perturbation  $\phi^{ext}(z; q, \omega)$ :

$$\delta n(z; q, \omega) = \int dz' \chi(z, z'; q, \omega) \phi^{ext}(z'; q, \omega), \quad (7)$$

$\chi(z, z'; q, \omega)$  representing the 2D Fourier transform of the density-response function of our *interacting* many-electron system.

The collective oscillations created by an external potential of the form<sup>15</sup>

$$\phi^{ext}(z; q, \omega) = -(2\pi/q) e^{qz} \quad (8)$$

can be traced to the peaks of the imaginary part of the so-called surface response function  $g(q, \omega)$ .<sup>16,17</sup>

$$g(q, \omega) = -\frac{2\pi}{q} \int dz \int dz' e^{q(z+z')} \chi(z, z'; q, \omega), \quad (9)$$

which at  $q = 0$  exhibits a pole at the conventional surface plasmon  $\omega_s$ .<sup>18</sup>

### A. Single-particle states

The starting point of our calculations is a set of single-particle states  $\psi_{\mathbf{k},n}(\mathbf{r})$  and energies  $E_{\mathbf{k},n}$  of the form

$$\psi_{\mathbf{k},n}(\mathbf{r}) = \frac{1}{\sqrt{A}} e^{i\mathbf{k}\cdot\mathbf{r}_{\parallel}} \phi_n(z) \quad (10)$$

and

$$E_{\mathbf{k},n} = \frac{k^2}{2m_n} + \varepsilon_n, \quad (11)$$

where  $\mathbf{r} \equiv (\mathbf{r}_{\parallel}, z)$ ,  $A$  is a normalization area, and  $\phi_n(z)$  and  $\varepsilon_n$  are the eigenfunctions and eigenvalues of a one-dimensional Schrödinger equation of the form

$$\left[ -\frac{1}{2} \frac{d^2}{dz^2} + V_{MP}(z) \right] \phi_n(z) = \varepsilon_n \phi_n(z), \quad (12)$$

$V_{MP}$  being the model potential described in Ref. 14. This potential reproduces the key features of the surface band structure, which in the case of the (111) surface of the noble metals are the presence of a band gap at the center of the 2D Brillouin zone (2DBZ) and the existence of Shockley and image states in it.

Alternatively, for a description of the screened interaction  $W(z, z'; q, \omega)$  entering Eqs. (2) and (6) (which accounts for the presence of 3D bulk states alone), the wave functions  $\phi_n(z)$  and  $\varepsilon_n$  can be taken to be the eigenfunctions and eigenvalues of a jellium Kohn-Sham Hamiltonian of density-functional theory (DFT),<sup>19</sup> which we evaluate in the local-density approximation (LDA) with the parametrization of Perdew and Zunger.<sup>20</sup>

In order to solve either Eq. (12) or the jellium Kohn-Sham equation of DFT, we consider a thick slab with a given number of atomic layers and assume that the electron density vanishes at a distance  $z_0$  from either crystal edge.<sup>21</sup> The one-dimensional wave functions  $\phi_n(z)$  are then expanded in a Fourier series of the form<sup>22</sup>

$$\phi_n(z) = \frac{1}{\sqrt{d}} c_{n,0}^+ + \frac{\sqrt{2}}{\sqrt{d}} \times \sum_{l=1}^{l_{max}} \left[ c_{n,l}^+ \cos\left(\frac{2\pi l}{d} z\right) + c_{n,l}^- \sin\left(\frac{2\pi l}{d} z\right) \right], \quad (13)$$

where the distance  $d$  is given by the equation

$$d = N d_0 + 2z_0, \quad (14)$$

$N$  and  $d_0$  being the number of atomic layers and the interlayer spacing, respectively; in the case of the (111) surfaces of the noble metals, we take  $N = 81$ ,  $z_0 = 10d_0$ , and  $l_{max}$  corresponding to an energy of 150 eV. Due to the symmetry of the model potential entering Eq. (12), the eigenfunctions  $\phi_n(z)$  are easily found to be either even ( $c_{n,l}^- = 0$ ) or odd ( $c_{n,l}^+ = 0$ ).

Figure 2 shows the energies  $E_{\mathbf{k},n}$  that we have obtained from Eq. (11) for Cu(111) by solving Eq. (12) as described above and using the experimental values of the effective masses  $m_n$  of all bulk and surface states. Electronic structures for Ag(111) and Au(111) are similar. The corresponding parameters are reported in Table I.

## B. Noninteracting density-response function

Once we have an accurate description of the single-particle orbitals  $\phi_n(z)$  and energies  $\varepsilon_n$ , we evaluate the 2D Fourier transform  $\chi^0(z, z'; q, \omega)$  of noninteracting electrons moving in either the model potential  $V_{MP}(z)$  or the jellium effective Kohn-Sham potential of DFT:

$$\chi^0(z, z'; q, \omega) = \frac{2}{A} \sum_{n,n'} \phi_n(z) \phi_{n'}(z) \phi_n(z') \phi_{n'}(z') \times \sum_{\mathbf{k}} \frac{f_{\mathbf{k},n} - f_{\mathbf{k}+\mathbf{q},n'}}{E_{\mathbf{k},n} - E_{\mathbf{k}+\mathbf{q},n'} + \omega + i\eta}. \quad (15)$$

Here, the sum over  $n$  and  $n'$  includes both occupied and unoccupied states,  $\eta$  is a positive infinitesimal, and  $f_{\mathbf{k},n}$  are Fermi factors, which at zero temperature are simply

given by the Heaviside step function

$$f_{\mathbf{k},n} = \Theta(\varepsilon_F - E_{\mathbf{k},n}), \quad (16)$$

$\varepsilon_F$  being the Fermi energy of the solid. In particular, the noninteracting density-response function of the quasi-2D band of occupied Shockley states in the absence of the 3D substrate can be obtained from Eq. (15) by omitting all bulk states in the sum over  $n$  and  $n'$ .

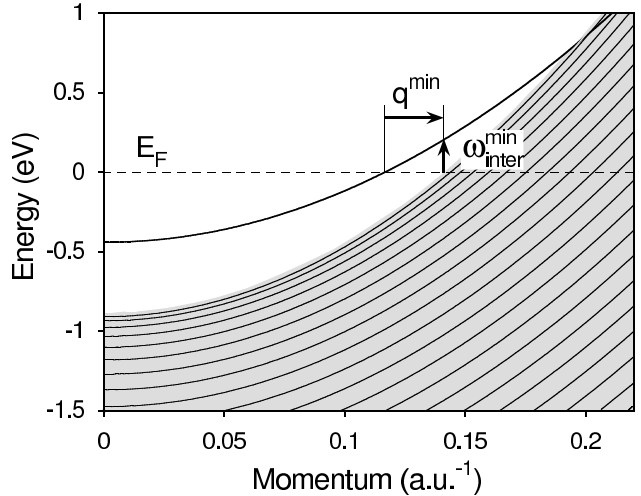


FIG. 2: Surface electronic structure of Cu(111). The thick solid line is the energy  $E_{\mathbf{k},n} = \varepsilon_F^{2D} + k^2/2m_{2D}$  of the Shockley surface state versus the 2D momentum  $k$ , as obtained with the measured value of the effective mass  $m_{2D}$ . The grey area (with the upper limit at  $E = \varepsilon_0 + k^2/2m_0$ ) represents the projected bulk band structure. The values of  $\varepsilon_F^{2D}$ ,  $m_{2D}$ ,  $\varepsilon_0$ , and  $m_0$  are reported in Table I. Solid lines correspond to the bulk states that we have obtained by employing a slab with 81 atomic layers to simulate the semi-infinite solid. We have used the following parameters in the description of the model potential  $V_{MP}$  entering Eq. (12):  $A_{10} = -11.805$ ,  $A_1 = 5.14$ ,  $A_2 = 4.4204$ , and  $\beta = 2.8508$  (for a description of the model potential see Ref. 14). Due to the presence of the band gap, for optical ( $q = 0$ ) transitions to occur from an occupied 3D bulk state to an unoccupied 2D surface state the minimum energy  $\omega_{inter}^{min}$  is required, which decreases as the momentum transfer  $q$  increases. For  $q$  larger than  $q^{min}$ , transitions from occupied (unoccupied) 3D bulk states to unoccupied(occupied) surface states can occur at arbitrary values of the energy transfer  $\omega$ .

Introducing the one-dimensional wave functions of Eq. (13) into Eq. (15), one finds the following Fourier representation of the noninteracting density-response function (see Appendix A):<sup>23</sup>

$$\chi^0(z, z'; q, \omega) = \sum_{n=0}^{\infty} \sum_{n'=0}^{\infty} \chi_{n,n'}^{0,+}(q, \omega) \cos\left(\frac{2\pi n}{d} z\right) \cos\left(\frac{2\pi n'}{d} z'\right) + \sum_{n=1}^{\infty} \sum_{n'=1}^{\infty} \chi_{n,n'}^{0,-}(q, \omega) \sin\left(\frac{2\pi n}{d} z\right) \sin\left(\frac{2\pi n'}{d} z'\right). \quad (17)$$

## C. Interacting density-response function

In the framework of the RPA,<sup>24</sup> the 2D Fourier transform  $\chi(z, z'; q, \omega)$  of the density-response function of an

interacting many-electron system is obtained by solving

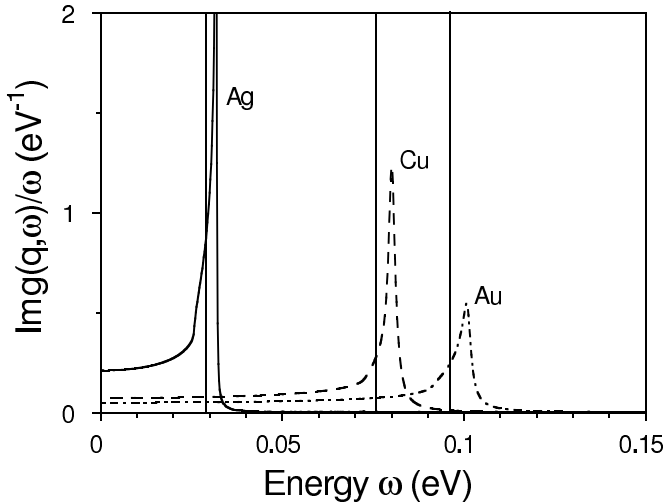


FIG. 3: Energy-loss function  $\text{Im}g(q, \omega)/\omega$  of the (111) surfaces of the noble metals Cu, Ag, and Au, shown by solid, dashed, and dashed dotted lines, respectively, versus the excitation energy  $\omega$ , as obtained from Eq. (9) for  $q = 0.01$  and  $\eta = 1$  meV. The vertical solid lines are located at the energies  $\omega = v_F^{2D} q$ , which would correspond to Eq. (3) with  $\alpha = 1$ .

the following integral equation

$$\chi(z, z'; q, \omega) = \chi^0(z, z'; q, \omega) + \int dz_1 \int dz_2 \chi^0(z, z_1; q, \omega) \times v(z_1, z_2; q) \chi(z_2, z'; q, \omega), \quad (18)$$

the ingredients of this equation being the 2D Fourier transforms  $\chi^0(z, z'; q, \omega)$  and  $v(z, z'; q)$  of the noninteracting density-response function and the bare Coulomb interaction, respectively. All quantities entering Eq. (18) can be represented in the form of Eq. (17), which yields the following matrix equation for the coefficients  $\chi_{m,n}^\pm(q, \omega)$ :

$$\chi_{n,n'}^\pm(q, \omega) = \chi_{n,n'}^{0,\pm}(q, \omega) + \sum_{n'',n'''} \chi_{n,n''}^{0,\pm}(q, \omega) \times v_{n'',n'''}(q) \chi_{n''',n'}^\pm(q, \omega), \quad (19)$$

$v_{n'',n'''}(q)$  being the corresponding coefficients of the bare Coulomb interaction  $v(z, z'; q)$ .

### III. RESULTS AND DISCUSSION

#### A. ASP dispersion

Figure 3 shows the energy-loss function  $\text{Im}g(q, \omega)$  of the (111) surfaces of the noble metals Cu, Ag, and Au, as obtained from Eq. (9) for  $q = 0.01$ . This figure shows the presence of a low-energy collective excitation, whose energy is of the form of Eq. (3) but with an  $\alpha$  coefficient that is close to unity. Furthermore, we have carried out calculations of  $\text{Im}g(q, \omega)$  for several low values of  $q$  and

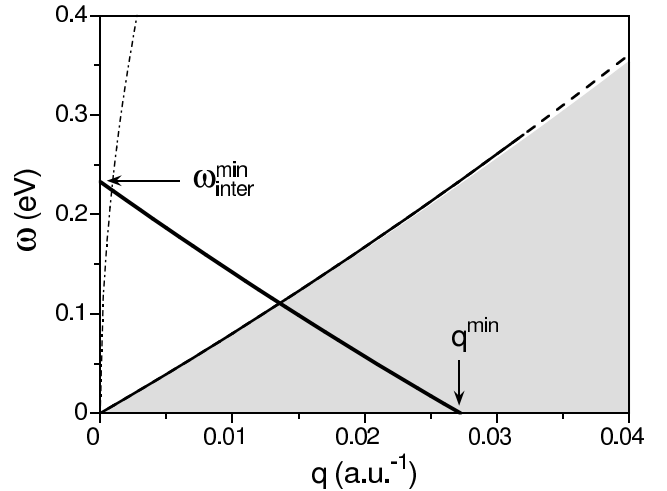


FIG. 4: The solid line shows the energy of a well-defined acoustic surface plasmon of Cu(111), as obtained from the maxima of our calculated surface-loss function  $\text{Im}g(q, \omega)$ . The dashed line represents the energy of an acoustic surface plasmon whose linewidth starts to be considerable due to the presence of interband transitions. The dashed dotted line is the plasmon dispersion of a 2D electron gas in the absence of the 3D system. The grey area indicates the region of the  $(q, \omega)$  plane (with the upper limit at  $\omega_{2D}^{\text{up}} = v_F^{2D} q + q^2/2m_{2D}$ ) where e-h pairs can be created within the 2D Shockley band of Cu(111). The area below the thick solid line corresponds to the region of momentum space where transitions between 3D and 2D states cannot occur. The quantities  $\omega_{\text{inter}}^{\text{min}}$  and  $q^{\text{min}}$  are determined from the surface band structure of Fig. 2.

we have found that this low-energy collective excitation is indeed an acoustic surface plasmon with linear dispersion, as shown in Fig. 4 for the case of Cu(111).

In Fig. 4, we show the energy of the acoustic surface plasmon of Cu(111) versus  $q$  (solid line), as derived from the maxima of our calculated  $\text{Im}g(q, \omega)$ , together with the well-defined plasmon energies that we obtain when only the surface-state band is considered in the evaluation of the noninteracting density-response function of Eq. (15) (dashed dotted line). While the plasmon energies of electrons in the isolated surface-state band nicely reproduce in the long-wavelength ( $q \rightarrow 0$ ) limit the conventional 2D plasmon dispersion  $\omega_{2D}$  of Eq. (1), the combination of this surface-state band with the underlying 3D system yields a *new* distinct mode whose energy lies just above the upper edge  $\omega_{2D}^{\text{up}} = v_F^{2D} q + q^2/2m_{2D}$  of the 2D e-h pair continuum, as occurs in the case of Be.<sup>8</sup> Furthermore, Fig. 4 shows that in the long-wavelength ( $q \rightarrow 0$ ) limit the energy of the acoustic surface plasmon in Cu(111) is of the form of Eq. (3) but with an  $\alpha$  coefficient that is considerably closer to unity than expected from Eq. (5) (see Table I). This discrepancy can be originated in (i) the absence in the simplified model leading to Eqs. (3) and (5) of transitions between 2D and 3D states, and (ii) the nature of the decay and penetration of the surface-state orbitals into the solid.

In order to investigate the origin of the small differ-

TABLE I: 2D Fermi energy ( $\varepsilon_F^{2D}$ ), effective mass ( $m_{2D}$ ), and Fermi velocity ( $v_F^{2D}$ ) of the Shockley surface-state band in the (111) surface of the noble metals Cu, Ag, and Au.  $\varepsilon_0$  represents the energy of the bottom of the gap at the  $\bar{\Gamma}$  point.  $m_0$  represents the effective mass of the upper bulk states at the bottom of the gap. The minimum energy transfer  $\omega_{\text{inter}}^{\text{min}}$  and momentum transfer  $q^{\text{min}}$  are those defined in Fig. 2. Also represented in this table are the values of the parameter  $\alpha$  that we have obtained from our full self-consistent calculations of the surface-response function of Eq. (9) and from Eq. (5) with  $z_d \ll 0$ .

	$\varepsilon_F^{2D}$ (meV)	$m_{2D}$	$v_F^{2D}$	$\varepsilon_0$ (eV)	$m_0$	$\omega_{\text{inter}}^{\text{min}}$ (meV)	$q^{\text{min}}$	$\alpha$	$\alpha$ [Eq. (5)]
Cu	440	0.42	0.277	-0.89	0.31	217	0.026	1.053	1.38
Ag	67	0.44	0.106	-0.4	0.25	160	0.039	1.042	1.41
Au	475	0.28	0.353	-1.0	0.21	275	0.025	1.032	1.41

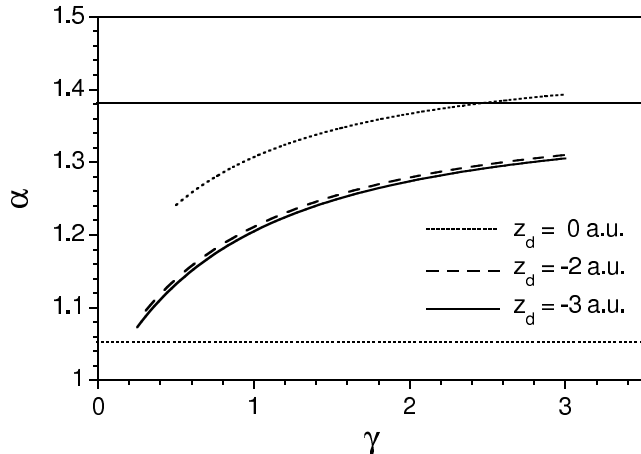


FIG. 5: In a simplified model in which the wave function of surface-state electrons decays exponentially away from the  $z = z_d$  plane (see Fig. 1) with a decay constant  $\gamma$ , acoustic surface plasmons are found to exist whose energy is of the form of Eq. (3) with the coefficient  $\alpha$  of Eq. (5) replaced by the  $\gamma$ -dependent  $\alpha$  coefficient that we have presented in this figure in the case of Cu(111) for various values of  $z_d$ . The horizontal solid line corresponds to the coefficient  $\alpha$  of Eq. (5) with  $z_d \ll 0$ . The horizontal dotted line represents the coefficient  $\alpha$  derived from our full self-consistent calculation that treats bulk and surface states on the same footing. As  $z_d$  is shifted from the interior of the solid towards the vacuum, the coefficient  $\alpha$  increases, in agreement with Ref. 9.

ences between the plasmon energies obtained here and those expected from Eqs. (3) and (5), we have carried out calculations of  $\text{Im}g(q, \omega)$  along the lines of the simplified model leading to Eqs. (3) and (5) (see Fig. 1) but with the 2D electron gas of Fig. 1 replaced by a more realistic quasi-2D gas of electrons described by a wave function that decays exponentially away from the  $z = z_d$  plane with a decay constant  $\gamma$ . We have found that an acoustic surface plasmon is present whose energy is indeed of the form of Eq. (3) but with an  $\alpha$  coefficient that strongly depends on the decay constant  $\gamma$ , as shown in Fig. 5. This figure demonstrates that while in the limit as  $\gamma \rightarrow \infty$  (where the quasi-2D electron gas is indeed an ideal 2D sheet) the coefficient  $\alpha$  approaches the value expected from Eq. (5) (horizontal solid line), as  $\gamma$  decreases the dispersion of the acoustic surface plasmon approaches

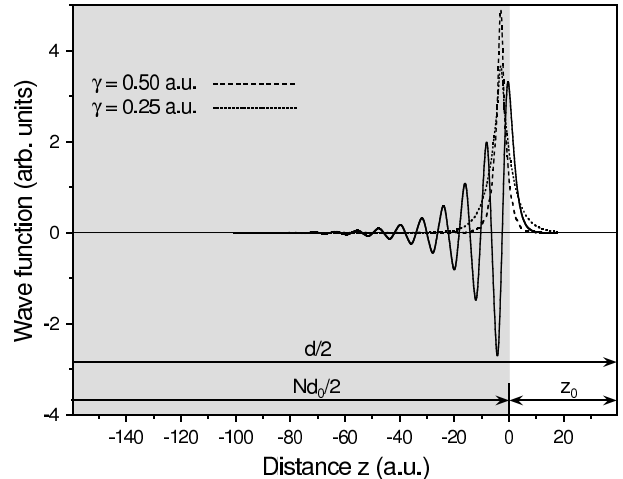


FIG. 6: The solid line is the wave function  $\phi(z)$  of the occupied Shockley surface state of Cu(111) at the  $\bar{\Gamma}$  point, as obtained by solving Eq. (12). The dashed and dotted lines show wave functions of the form  $\phi(z) \sim \exp(-\gamma|z - z_d|)$  with  $z_d = -3$  a.u. and two different values of the decay constant:  $\gamma = 0.5 a_0^{-1}$  (dashed line) and  $\gamma = 0.25 a_0^{-1}$  (dotted line).  $a_0$  is the Bohr radius:  $a_0 = 0.529 \text{ \AA}$ .

(for all negative values of  $z_d$ ) the more realistic situation where  $\alpha$  is close to unity (horizontal dotted line). A comparison between the model wave functions that we have used in this calculation and the actual surface-state wave functions that are involved in the full calculation of Figs. 3 and 4 is presented in Fig. 6. Although the *model* wave functions do not reproduce the actual shape of the surface-state wave function, a finite penetration of the model surface-state wave functions into the solid allows the formation of an acoustic surface plasmon whose sound velocity is very close to the Fermi velocity of the 2D surface-state band ( $\alpha \sim 1$ ), as predicted by our more realistic calculation. Indeed, the finite penetration of the surface-state wave function into the solid provides a more complete screening of the quasi-2D collective excitations by the surrounding 3D substrate, which brings the acoustic surface plasmon closer to the upper edge of the 2D e-h pair continuum ( $\alpha \rightarrow 1$ ).<sup>25</sup>

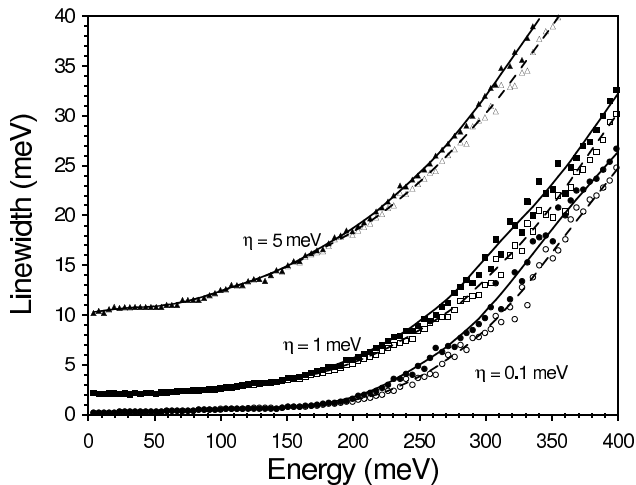


FIG. 7: Solid and open symbols represent the width at half maximum of acoustic surface plasmons in Cu(111) versus the plasmon energy, as obtained from the imaginary part of the surface-response function  $g(q, \omega)$  of Eq. (9) with (solid symbols) and without (open symbols) inclusion of transitions between 2D and 3D states in the evaluations of the noninteracting density-response function of Eq. (15) and for various values of the parameter  $\eta$ : 0.1, 1, and 5 meV. The solid and dashed lines represent fits from the solid and open symbols, respectively. For this surface, the threshold for interband transitions between 2D and 3D states occurs at  $\sim 110$  meV (see Fig. 4).

### B. ASP linewidth

Finally, we have carried out lifetime calculations of the acoustic surface plasmon, as derived from the width of the imaginary part of the full surface-response function of Eq. (9). Fig. 7 shows the results we have obtained for Cu(111) with (solid symbols and lines) and without (open symbols and dashed lines) inclusion of transitions between 2D and 3D states in the evaluation of the noninteracting density-response function of Eq. (15) and for three different values of the parameter  $\eta$ . Plasmon decay can occur by exciting e-h pairs either through transitions between 2D and 3D states, which would not be present in the model leading to Eqs. (3) and (5), or through transitions within the 3D continuum of bulk states.<sup>26</sup> At small energies below the threshold of  $\omega \sim 110$  meV (see Fig. 4), where acoustic surface plasmons can only decay by exciting e-h pairs within the 3D continuum of bulk states (the solid and dashed lines of Fig. 7 coincide), the linewidth is entirely determined by the choice of the parameter  $\eta$ , showing that at these low energies the impact of intraband transitions between 3D bulk states is negligibly small. As the plasmon energy increases, there is a small contribution to the plasmon linewidth from transitions between 2D and 3D states (the difference between solid and dashed lines)<sup>27</sup> and an increasing contribution from intraband 3D transitions yielding a finite linewidth which for  $\eta < 0.1$  eV is not sensitive to the precise value of  $\eta$  employed, but which still allows the formation of a well-

defined acoustic-surface collective excitation for plasmon energies at least up to  $\sim 400$  meV. A similar behavior is observed in the case of Ag and Au.

## IV. SUMMARY AND CONCLUSIONS

We have carried out self-consistent calculations of the surface-loss function of the (111) surfaces of the noble metals Cu, Ag, and Au, by considering a one-dimensional potential that describes the main features of the surface band structure. We have found that the partially occupied surface-state band in these materials yields the existence of acoustic surface plasmons, as it had already been demonstrated to occur in the case of Be(0001).<sup>8</sup> The energy of these collective excitations has been shown to exhibit linear dispersion at small wave vectors, with the sound velocity being very close to the Fermi velocity of the 2D surface-state band and considerably smaller than expected from a simplified model in which surface-state electrons comprise a 2D electron gas while all other states of the semi-infinite metal comprise a 3D substrate.

The origin of the differences between the plasmon energies obtained here and those expected from simplified models has been investigated by performing simplified calculations with the ideal 2D sheet of Shockley electrons replaced by a more realistic quasi-2D gas of electrons whose wave functions decay exponentially away from the surface. These calculations have been found to yield an acoustic surface plasmon whose energy is linear in the magnitude of the wave vector, the sound velocity being dictated not only by the Fermi velocity of the 2D surface-state band but also by the nature of the decay and penetration of the surface-state orbitals into the solid. With an appropriate choice of the exponential decay of surface-state wave functions these simplified calculations (which do not account for transitions between 2D and 3D states) accurately account for the energy dispersion of acoustic surface plasmons, which indicates that the impact of interband transitions between 2D and 3D states on the ASP's energy dispersion is negligible.

We have also carried out self-consistent calculations of the linewidth of acoustic surface plasmons in the (111) surfaces of the noble metals. We have found that while the impact of interband transitions between 2D and 3D states is small, intraband transitions between 3D bulk states contribute considerably to the finite linewidth of acoustic surface plasmons, which are found to represent a well-defined acoustic collective excitation for plasmon energies at least up to  $\sim 400$  meV.

Finally, we note that as in the case of conventional surface plasmons, acoustic surface plasmons should also be expected to be excited by light, as discussed recently.<sup>28</sup>

## V. ACKNOWLEDGMENTS

We gratefully acknowledge partial support by the University of the Basque Country, the Basque Unibertsitate eta Ikerketa Saila, the Spanish Ministerio de Ciencia y Tecnología, and the EC 6th framework Network of Excellence NANOQUANTA (NMP4-CT-2004-500198).

## APPENDIX A

Here we give explicit expressions for the coefficients  $\chi_{n,n'}^{0,\pm}(q,\omega)$  entering the expansion of the noninteracting

density-response function of Eq. (17), as obtained by introducing the one-dimensional wave functions of Eq. (13) into Eq. (15). Replacing the sum over  $\mathbf{k}$  in Eq. (15) by an integral, we find

$$\chi_{n,n'}^{0,+}(q,\omega) = \frac{\delta_n \delta_{n'}}{d^2} \left\{ \sum_{l_{\text{even}} l'_{\text{even}}}^{\text{occ}} \sum_{l_{\text{odd}} l'_{\text{odd}}}^{\infty} F_{l,l'}(q,\omega) G_{n;l,l'}^{++} G_{n';l,l'}^{++} + \sum_{l_{\text{odd}} l'_{\text{odd}}}^{\text{occ}} \sum_{l_{\text{even}} l'_{\text{even}}}^{\infty} F_{l,l'}(q,\omega) G_{n;l,l'}^{--} G_{n';l,l'}^{--} \right\} \quad (\text{A1})$$

and

$$\chi_{n,n'}^{0,-}(q,\omega) = \frac{4}{d^2} \left\{ \sum_{l_{\text{even}} l'_{\text{odd}}}^{\text{occ}} \sum_{l_{\text{odd}} l'_{\text{even}}}^{\infty} F_{l,l'}(q,\omega) G_{n;l,l'}^{+-} G_{n';l,l'}^{+-} + \sum_{l_{\text{odd}} l'_{\text{even}}}^{\text{occ}} \sum_{l_{\text{even}} l'_{\text{odd}}}^{\infty} F_{l,l'}(q,\omega) G_{n;l,l'}^{-+} G_{n';l,l'}^{-+} \right\}, \quad (\text{A2})$$

where

$$\delta_n = \begin{cases} 1, & \text{for } n = 0 \\ 2, & \text{for } n \geq 1 \end{cases} \quad (\text{A3})$$

and

$$F_{l,l'}(q,\omega) = \int dk k \left[ F_{l,l'}^+(q,k,\omega) - F_{l,l'}^-(q,k,\omega) \right], \quad (\text{A4})$$

with

$$F_{l,l'}^{\pm}(q,k,\omega) = \theta \left( \varepsilon_F - \epsilon_l - \frac{k^2}{2m_l} \right) \left[ \frac{q^2 k^2}{m_l^2} - \left( \frac{q^2}{2m_{l'}} + \epsilon_{l'} - \epsilon_l + \frac{k^2}{2m_{l'}} - \frac{k^2}{2m_l} \pm \omega \pm i\eta \right)^2 \right]^{-1/2}, \quad (\text{A5})$$

$$G_{n;l,l'}^{++} = c_{l,0}^+ c_{l',0}^+ \delta_{n,0} + \frac{1}{\sqrt{2}} \sum_{n' \neq 0} (c_{l,n'}^+ c_{l',0}^+ + c_{l,0}^+ c_{l',n'}^+) \delta_{n,n'} + \frac{1}{2} \sum_{n' \neq 0} \sum_{n'' \neq 0} c_{l,n'}^+ c_{l',n''}^+ (\delta_{n+n'',n'} + \delta_{n+n',n''} + \delta_{n'+n'',n}), \quad (\text{A6})$$

$$G_{n;l,l'}^{--} = \frac{1}{2} \sum_{n' \neq 0} \sum_{n'' \neq 0} c_{l,n'}^- c_{l',n''}^- (\delta_{n+n'',n'} + \delta_{n+n',n''} - \delta_{n'+n'',n}), \quad (\text{A7})$$

$$G_{n;l,l'}^{+-} = \frac{1}{\sqrt{2}} c_{l,0}^+ c_{l',n}^- + \frac{1}{2} \sum_{n' \neq 0} \sum_{n'' \neq 0} c_{l,n'}^+ c_{l',n''}^- (-\delta_{n+n'',n'} + \delta_{n+n',n''} + \delta_{n'+n'',n}), \quad (\text{A8})$$

and

$$G_{n;l,l'}^{-+} = \frac{1}{\sqrt{2}} c_{l,n}^- c_{l',0}^+ + \frac{1}{2} \sum_{n' \neq 0} \sum_{n'' \neq 0} c_{l,n'}^- c_{l',n''}^+ (\delta_{n+n'',n'} - \delta_{n+n',n''} + \delta_{n'+n'',n}). \quad (\text{A9})$$

- 
- <sup>1</sup> J. E. Inglesfield, Rep. Prog. Phys. **45**, 223 (1982).
- <sup>2</sup> S. Hüfner, Photoelectron Spectroscopy - Principles and Applications, vol. 82 of Springer Series in Solid-state Science, Springer, Berlin, 1995.
- <sup>3</sup> H. Nienhaus, Surf. Sci. Rep. **45**, 1 (2002).
- <sup>4</sup> P. M. Echenique, R. Berndt, E. V. Chulkov, Th. Fauster, A. Goldmann, U. Höfer, Surf. Sci. Rep. **52**, 219 (2004).
- <sup>5</sup> F. Stern, Phys. Rev. Lett. **18**, 546 (1967); T. Ando, A. B. Fowler, and F. Stern, Rev. Mod. Phys. **54**, 437 (1982).
- <sup>6</sup> T. Nagao, T. Heldebrandt, M. Henzler, and S. Hasegawa, Phys. Rev. Lett. **86**, 5747 (2001).
- <sup>7</sup> N. H. March and M. P. Tosi, Adv. Phys. **44**, 299 (1995).
- <sup>8</sup> V. M. Silkin, A. García-Lekue, J. M. Pitarke, E. V. Chulkov, E. Zaremba, and P. M. Echenique, Europhys. Lett. **66**, 260 (2004).
- <sup>9</sup> J. M. Pitarke, V. U. Nazarov, V. M. Silkin, E. V. Chulkov, E. Zaremba, and P. M. Echenique, Phys. Rev B **70**, 205403 (2004).
- <sup>10</sup> R. H. Ritchie, Phys. Rev. **106**, 874 (1957).
- <sup>11</sup> See, e.g., P. M. Echenique, J. M. Pitarke, E. V. Chulkov, and A. Rubio, Chem. Phys. **251**, 1 (2000).
- <sup>12</sup> If one characterizes the 3D substrate by a local dielectric function, the characteristic collective oscillations of the 2D electron gas would be completely screened by the surrounding 3D substrate and no low-energy acoustic mode would exist for a 2D sheet inside the 3D substrate, i.e., for  $z_d \leq 0$ . This result has suggested over the years that acoustic plasmons should only exist in the case of *spatially separated* plasmas, as pointed out by Das Sarma and Madhukar [S. Das Sarma and A. Madhukar, Phys. Rev. B **23**, 805 (1981)].
- <sup>13</sup> This is precisely the result first obtained by Chaplik [A. V. Chaplik, Zh. Eksp. Teor. Fiz. **62**, 746 (1972) (Sov. Phys. JETP, **35**, 395 (1972))] in his study of charge-carrier crystallization in low-density inversion layers, by assuming that both the 3D and 2D subsystems can be characterized by local dielectric functions of the Drude form.
- <sup>14</sup> E. V. Chulkov, V. M. Silkin, and P. M. Echenique, Surf. Sci. **391**, L1217 (1997); **437**, 330 (1999).
- <sup>15</sup> This would be the potential created by, e.g., electrons moving far from the metal in the vacuum side of the surface.
- <sup>16</sup> P. J. Feibelman, Prog. Surf. Sci. **12**, 287 (1982).
- <sup>17</sup> B. N. J. Persson and E. Zaremba, Phys. Rev. B **31**, 1863 (1985).
- <sup>18</sup> See, e.g., A. Liebsch, *Electronic Excitations at Metal Surfaces* (Plenum Press, New York, 1997).
- <sup>19</sup> P. Hohenber and W. Kohn, Phys. Rev. **136** B864 (1964); W. Kohn and L. J. Sham, Phys. Rev. A **1133** (1965).
- <sup>20</sup> J. P. Perdew and A. Zunger, Phys. Rev. B **23**, 5048 (1981).
- <sup>21</sup> The crystal edge is taken to be half an interlayer spacing beyond the last atomic layer.
- <sup>22</sup> The vacuum distance  $z_0$  and the upper limit  $l_{max}$  are chosen sufficiently large for the physical results to be insensitive to the precise value employed.
- <sup>23</sup> A similar double-cosine Fourier representation was introduced by Eguiluz [A. G. Eguiluz, Phys. Rev. Lett. **51**, 1907 (1983)] to evaluate the density-response function of free electrons in a jellium surface.
- <sup>24</sup> A. L. Fetter and J. D. Wallecka, *Quantum Theory of Many-Particle Systems* (McGraw-Hill, New York, 1964).
- <sup>25</sup> If the 2D collective excitations were completely screened by the 3D substrate, no low-energy acoustic mode would exist, as shown in Ref. 9.
- <sup>26</sup> Since the 3D Fermi velocity  $v_F^{3D}$  of the noble metals is larger than the Fermi velocity  $v_F^{2D}$  of the corresponding 2D surface-state band, acoustic surface plasmons can always decay by exciting e-h pairs within the 3D continuum of bulk states.
- <sup>27</sup> This contribution to the plasmon linewidth is small due to the small coupling between 2D and 3D orbitals.
- <sup>28</sup> J. M. Pitarke, V. M. Silkin, E. V. Chulkov, and P. M. Echenique, J. of Optics A: Pure and Appl. Opt. **7**, S73 (2005).